CHEMICAL ENGINEERING TRANSACTIONS
VOL. 87, 2021
A publication of AIDIC
The Italian Association of Chemical Engineering
Online at www.aidic.it/cet
Guest Editors: Laura Piazza, Mauro Moresi, Francesco Donsì

ISBN 978-88-95608-85-3; **ISSN** 2283-9216

Flexible electrode based on gold nanoparticles and reduced graphene oxide for uric acid detection using linear sweep voltammetry

Francesca Mazzara*[a], Bernardo Patella[a], Fabrizio Ganci[a], Alan O'Riordan[b], Giuseppe Aiello[a], Claudia Torino[c], Antonio Vilasi[c], Carmelo Sunseri[a], Rosalinda Inguanta[a]

[a]Laboratorio Chimica Fisica Applicata, Dipartimento di Ingegneria, Università degli Studi di Palermo, Viale delle Scienze, 90128 Palermo
[b]Nanotechnology group, Tyndall National Institute, University College Cork, Dyke Prade, Cork, Ireland
[c]Istituto di Fisiologia Clinica (IFC)-Consiglio Nazionale delle Ricerche-Reggio Calabria-Italy
*francesca.mazzara04@unipa.it

In this work, an electrochemical sensor for uric acid determination is shown with a preliminary study for its validation in real samples (milk and urine). Uric acid can be electrochemically oxidized in aqueous solutions and thus it is possible to obtain electrochemical sensors for this chemical by means of this electrooxidation reaction. Indium tin oxide coated on flexible polyethylene terephthalate substrate, modified with reduced graphene oxide and gold nanoparticles by co-electrodeposition, was used. Electrodeposition was performed at -0.8V vs SCE for 200 s. All samples were characterized by electron scan microscopy and electron diffraction spectroscopy. A careful investigation on the effect of pH was performed to understand its influence on uric acid oxidation. The detection of uric acid was using the linear sweep voltammetry. Results show that the peak current increases linearly with uric acid concentration from 10 to 1000 µM with a limit of detection of about 7.1 µM. The sensor shows high selectivity towards different interferents that can be found in the milk and urine matrix, such as chloride, calcium, sodium and ammonium ions. To prove the applicability of the proposed sensor, uric acid was quantified in real milk and urine samples with excellent results comparable to those of conventional techniques.

1. Introduction

In the last decades, the use of electrochemical sensors has rapidly increased in various research fields, such as environmental, health and food-safety. The use of sensors allows quantifying the presence of specific analytes in a simple, fast, reliable and economical way. Uric acid (UA) is a heterocyclic compound and is a natural waste product of the metabolic breakdown of purines, molecules that are found in DNA and RNA. Purine content in the human body can be both endogenous and exogenous. It can be produced by the body or they can lead from diet. Many food and drinks that are part of a normal diet contain purines and in some of these, the concentration is high, such as meats, seafood especially sardines, dried beans, beer (Xia et al., 2018). Purines are metabolized into uric acid and excreted by urine. In human blood and urine, normal levels of UA are 0.14 ÷ 0.4 mM (INSERM, 2020) and 1.5 ÷ 4.5mM (Yazdani et al., 2015) respectively, but many factors can affect these values such as age and gender (Nasri, 2016). Altered UA concentrations in the human body have been linked to many diseases. In particular, high levels in blood plasma causes hyperuricemia, that leads gout disease, a type of arthritis resulting from precipitation of small needle-like crystals in the joints (Hidayat et al., n.d.). Hyperuricemia Increases the risk for cardiovascular disease (Kuwabara, 2016), and causes the Lesch–Nyhan syndrome (Nyhan, 2007), and type 2 diabetes (Dehghan et al., 2008). On the other hand, low levels of

UA can be related to multiple sclerosis, Parkinson's and Alzheimer's diseases (Alonso and Sovell, 2010; Jin Jun Luo, 2013).
For all these reasons, it is important to evaluate UA concentration in food, beverage and body fluids. For UA detection different methods have been employed including complexometric and titrimetric methods, liquid chromatography and spectrophotometric (Okiei et al., 2009). UA can be easily electrochemically oxidized in aqueous solutions, for this reason electrochemical techniques such as cyclic voltammetry, differential pulse voltammetry and amperometry have been also used. Due to their fast and sensitive responses, electrochemical techniques seem to be a valid, simple and reliable method. In particular it was showed that graphene-based sensors are very versatile and efficient. In fact, graphene is a suitable material for electrochemical sensors because of its excellent electrical, thermal and optical properties. It has a high surface to volume ratio, abundant defects and fast electron transfer rates (Lee et al., 2019). An approach to detection of UA has been developed by fabrication of graphene-modified carbon fibre electrode (GE/CFE). Du et al. (Du et al., 2013) showed that the combined effect of GE and CFE ensures a large electrode specific surface area and high electrical conductivity. To improve the electrochemical performance of graphene, Rezaei et al (Rezaei et al., 2018) developed an electrochemical sensor based on zinc oxide and graphene oxide (ZnO/GR) modifying graphite screen-printed electrode (SPE). Graphene was also coupled with other nanoparticles (NPs) that have unique structural properties. In particular, NPs accelerate electron transfer and reduce overvoltage of electrochemical process. NPs of noble metal possess several unique catalytic and electronic properties, and have been tested for a lot of application, particularly for sensing. For example, a glassy carbon electrode was modified with electrodeposited gold nanoparticles (Au/GCE) and used to electrochemical detection of UA under visible light illumination (xenon lamp).With this system, Shi et al. (Shi et al., 2017) observed not only an increase in peak current detection but also a major stability respect to tests carried out without illumination. Xue et al. (Xue et al., 2011) synthesized and characterized three types of gold nanoparticles/graphene nanosheets (AuNPs/GNs) hybrid nanocomposites obtained by one-pot synthesis (AuNPs/GNs-P), in situ reduction (AuNPs/GNs-R) and absorption method (AuNPs/GNs-A). The electrocatalytic activity of these electrodes towards the oxidation of UA has been studied by CV analysis. With respect to the bare electrode, all three types of sensor show a higher peak current. In particular, AuNPs/GNs-A leads a considerable increase in anodic peak current of about 41.7 times than the bare electrode.
The main issue in the development of an electrochemical sensor for uric acid concerns its selectivity. Particularly, ascorbic acid (AA) and dopamine (DA) are considered the main interferents (Wu et al., 2020) (Temmer et al., 2013) due to their similar peak potentials. To overcome this problem, Tukimin et al. (2017) developed an electrochemical sensor based on poly(3,4-ethylene dioxythiophene)/reduced graphene oxide electrode for UA detection in presence of AA. This sensor shows good selectivity. In fact, the UA and AA peaks appear separated and well-defined located at 0.38 and 0.19 mV respectively, instead, they are not distinguished in the bare GCE electrode.
In this work, a flexible electrochemical sensor was developed by simple co-electrodeposition of reduced graphene oxide (rGO) and gold nanoparticles (AuNPs) on ITO-PET substrate. Chemical composition and morphology were determined by EDS and SEM analyses. Because the redox reaction of UA highly depends on pH, a study to investigate the effect of pH solution on UA detection was carried out. The calibration curve was obtained by employing a nitrate buffer solution ($NaNO_3$) at pH 8. To understand the applicability of the as-produced electrode to real samples, interference tests were performed toward the most common species. Finally, sensors were validated with real samples (milk and urine) obtaining good and reliable results.

2. Experimental

2.1 Electrode Fabrication

ITO-PET sheets were employed as a substrate and modified by simple electrochemical co-deposition of rGO and AuNPs. The production procedure for co-electrodeposition is detailed in (Mazzara et al., 2020.; Patella et al., 2019). The composition of deposition solution is reported in Table 1. The ITO-PET substrate was sonically washed with pure iso-propanol and distilled water for five minutes, respectively. The deposition solution was prepared using acetate buffer and the process was performed at room temperature. The electrodeposition was carried out for 200 seconds at a constant potential of -0.8 V vs SCE. Electrodeposition and electrochemical characterization were performed in 1 ml holder developed employing a Zortrax 3D printer. The deposition area is about 0.79 cm^2. All chemicals were purchased from Sigma-Aldrich and used without further purification except when mentioned specifically. Electrochemical measurements were performed with PARSTAT electrochemical workstation. Morphology was investigated using a FEG-ESEM microscope (model: QUANTA 200 by FEI), equipped with Energy Dispersive Spectroscopy (EDS) probe. All tests reported in this work was repeated three times using a new electrode and fresh solution for each.

Table 1: Main conditions for the co-electrodeposition of rGO-AuNPs.

Parameter	Value
$KAuCl_4$	0.25 mM
GO	0.5 mg/ml
Deposition time	200 s
Deposition potential	-0.8 V vs SCE
pH	5

2.2 Electrochemical detection

The electrochemical oxidation of UA strictly depends on the pH of the detection solution. Thus, in order to found the best sensing condition, UA detection was optimized in the pH range from 7 to 9. UA detection was performed by Linear Sweep Voltammetry (LSV). All experiments were conducted in a three-electrode cell employing standard calomel electrode (SCE) as reference, Pt wire as counter and ITO-rGO-AuNPs as working electrode. The calibration curve was obtained by employing the subtract baseline method. With the aim to prove the applicability of the as-produced electrode to real samples, the interference test was also performed. Particularly, interference of the most common body fluids and foodstuff ions (chloride, calcium, sodium and ammonium ions) was studied. Finally, sensors were validated with real samples (milk and urine) to compare our results with those obtained with conventional techniques. All measurements were performed in triplicate and the main value of these has been plotted to calculate the main properties of the sensor.

3. Results and Discussion

3.1 Characterization of ITO-rGO-AuNPs electrode

Figure 1a shows the current density ($\mu A/cm^2$) vs time curve reordered during the co-deposition of graphene oxide and gold-nanoparticles at a potential of 0.8 V vs SCE. As it is possible to observe, after an initial transient (after just 100 seconds), the curve reaches a plateau of about -50 $\mu A\ cm^{-2}$. For each obtained electrode, the growth curve is almost the same suggesting a good reproducibility of obtained samples. These deposition conditions were selected after a previously optimization of the different parameters of electrodeposition process, described in detail in our previous work (Patella et al., 2019). In particular these conditions allowed to obtain an electrode with specific surface morphology characterized by a high electrochemical active surface area. The co-deposition of rGO and Au was confirmed by EDS analysis, reported in Figure 1b. In particular, the presence of characteristic Au peak proves the deposition of gold. The carbon peak comes from both rGO and ITO substrate. Indium and tin peaks, instead, arise from the ITO substrate.

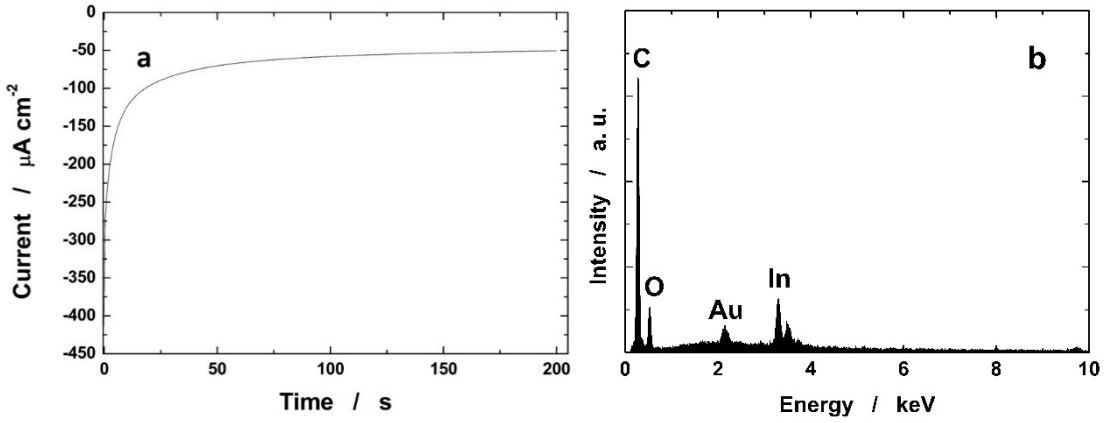

Figure 1: a) Current-time co-electrodeposition of rGO and AuNPs; b) EDS analysis of ITO-rGO-AuNPs electrode.

Figure 2 shows the typical SEM images of the sample surface. These images exhibit the presence of rGO sheets on which is clear the deposition of AuNPs with a main diameter of about 20 nm. The gold NPs are found on the entire surface of the electrode even if a greater densification can be noticed in the edges of the graphite sheets.

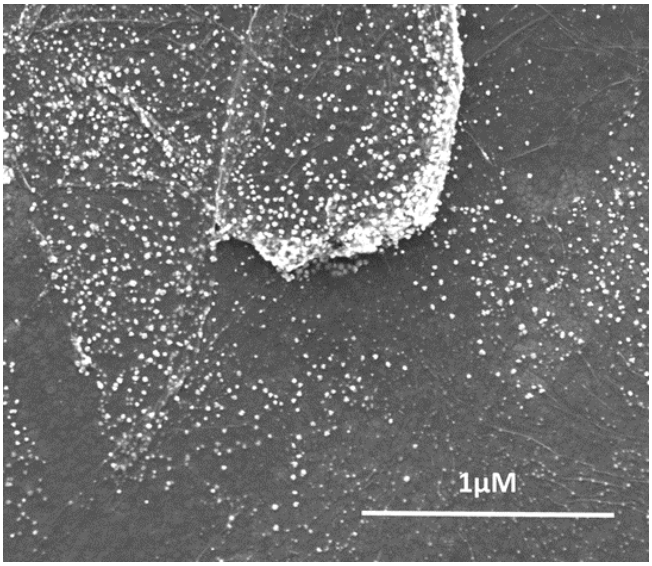

Figure 2: SEM image of ITO-rGO-AuNPs.

3.2 Electrochemical characterization

In Figure 3 the electrochemical oxidation of 100 µM UA dissolved in $NaNO_3$ solution at different pH from 7 to 9 was reported. The studies carried out on pH effect allowed to understand the relationship among peak potential and pH values. Although peak current intensity at pH 7 appears slightly more intense, the best result in terms of reproducibility were obtained at pH 8. As shown in the inset of figure as the pH increases from 7 to 9, peak potential decreases. The slope of linear regression is close to theoretical Nernst value of -59 mV/pH unit.

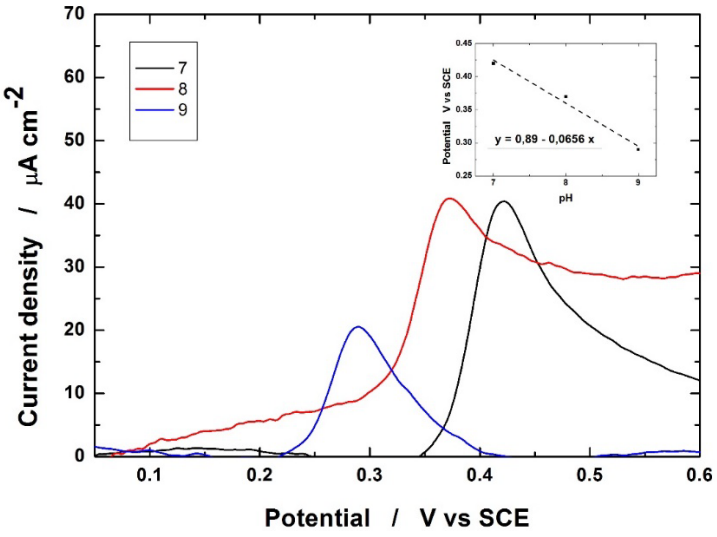

Figure 3: Effect of pH of $NaNO_3$ on UA detection on ITO-rGO-AuNPs electrode

LSV technique has been used to investigate UA concentration in a range from 10 to 1500 µM. A typical LSV curve for the oxidation of UA on ITO-rGO-AuNPs surface is shown in Figure 4. The UA peak can be easily identified at about 0.4 V vs SCE. It starts to appear for 10 µM concentration and linearly increased up to 500 µM with a sensitivity of 0.17 µA $\mu M^{-1}cm^{-2}$ and R^2 of 0.994. Limit of detection (LOD) and limit of quantification (LOQ) were calculated by using the following equations.

$$LOD = 3.3\ SD\ S^{-1}$$
$$LOQ = 10\ SD\ S^{-1}$$

in which SD is the standard deviation of the blank and S is the sensitivity of the electrode. Using these equations, a LOD and LOQ of 3.6 and 10.95 µM respectively was measured.

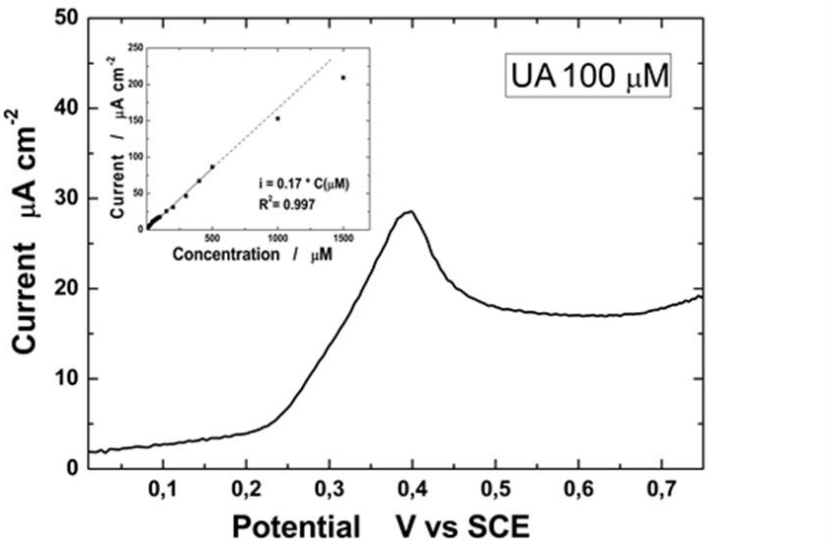

Figure 4: LSV for the oxidation of 100 µM UA on ITO-rGO-AuNPs surface and calibration line

Interference tests were performed toward different species present in real sample, to understand the applicability of the here obtained electrodes. A solution of 100 µM UA was used containing also the most common interfering species present in body fluids and foodstuff such as chloride, sodium and ammonium ions and ascorbic acid in a concentration of at least one to ten times higher than UA. The results obtained showed a negligible interference effect on the detection of UA. In fact, the peak potential of UA oxidation remains stable at 0.4 V vs SCE. Finally, real milk and urine sample has been tested and preliminary results appear in good agreement with literature data.

4. Conclusions

In this work, ITO-rGO-AuNPs electrodes were fabricated by co-electrodeposition technique for UA detection. The method employed for the electrode fabrication, which is in general simple and cheap, also proved effective for the deposition of rGO sheets and AuNPs on ITO-PET substrate. After the fabrication, the electrode was chemically and morphologically characterized with EDS and SEM analyses. Because the redox reaction of UA highly depends on pH, a study to investigate the effect of pH solution on UA detection was carried out. Calibration curve was obtained by employing nitrate solution ($NaNO_3$) at pH 8. A linear range from 10 to 500 µM was obtained with R^2 of 0.994 and sensitivity of 0.17 µA $\mu M^{-1} cm^{-2}$. LOD and LOQ were calculated founding about 3.6 and 10.95 µM respectively. The interference tests showed an excellent selectivity of the proposed sensor even at 1:10 ratio of UA/interferant. Finally, preliminary tests were carried out to detect the UA in real samples of milk and urine with appreciable results. Further work is in progress aimed to fabricate and test ITO-rGO-AuNPs electrode able to detect UA and AA concentration simultaneously.

Acknowledgments

This work was supported by University of Palermo and Italian National Research Council, and has been partially financed by the Project “PATCHES – Patient-Centered HEalthcare System for neurodegenerative diseases” (n. 610, Ministero dello Sviluppo Economico, Accordi per l’innovazione, Programma operativo nazionale «Imprese e competitività» 2014-2020 FESR e del Fondo per la crescita sostenibile).

References

Alonso A., Sovell K.A., 2010, Gout, Hyperuricemia, and Parkinson's Disease: A Protective Effect?, Current Rheumatology Reports, 12, 149–155.

Dehghan A., Van Hoek M., Sijbrands E.J.G., Hofman A., Witteman J.C.M., 2008, High Serum Uric Acid as a Novel Risk Factor for Type 2 Diabetes, Diabetes Care, 31, 361–362.

Du J., Yue R., Yao Z., Jiang F., Du Y., Yang P., Wang C., 2013, Nonenzymatic uric acid electrochemical sensor based on graphene-modified carbon fiber electrode, Colloids and Surfaces A: Physicochemical and Engineering Aspects, 419, 94–99.

Hidayat I., Hamijoyo L., Moeliono M., n.d., A survey on the clinical diagnosis and management of gout among general practitioners in Bandung, 04, 6.

INSERM, 2020. Phosphoribosylpyrophosphate synthetase superactivity, in: Definitions. Qeios.

Jin Jun Luo, X.L., 2013. A Double-edged Sword: Uric Acid and Neurological Disorders, Brain Disorders & Therapy 02.

Kuwabara M., 2016, Hyperuricemia, Cardiovascular Disease, and Hypertension, Pulse, 3, 242–252.

Lee J.-H., Park S., Choi J.-W., 2019, Electrical Property of Graphene and Its Application to Electrochemical Biosensing. Nanomaterials, 9, 297.

Mazzara F., Patella B., Aiello G., Sunseri C., Inguanta R., n.d, Ascorbic Acid determination using linear sweep voltammetry on flexible electrode modified with gold nanoparticles and reduced graphene oxide, 2020 IEEE 20th Mediterranean Electrotechnical Conference (MELECON), 406-410.

Nasri H., 2016, Uric acid is an index of chronic diseases or is an index of antioxidant? A mini-review to the recent trends, 2, 4.

Nyhan W.L., 2007, Lesch-Nyhan Disease and Related Disorders of Purine Metabolism, Tzu Chi, Medical Journal, 19, 105–108.

Okiei W., Ogunlesi M., Azeez L., Obakachi V., Osunsanmi M., Nkenchor G., 2009, The Voltammetric and Titrimetric Determination of Ascorbic Acid Levels in Tropical Fruit Samples, International Journal of Electrochemical Science, 4, 12.

Patella B., Sortino A., Aiello G., Sunseri C., Inguanta R., 2019, Reduced graphene oxide decorated with metals nanoparticles electrode as electrochemical sensor for dopamine, 2019 IEEE International Conference on Flexible and Printable Sensors and Systems (FLEPS), 1–3.

Rezaei R., Foroughi M.M., Beitollahi H., Alizadeh R., 2018, Electrochemical Sensing of Uric Acid Using a ZnO/Graphene Nanocomposite Modified Graphite Screen Printed Electrode, Russian Journal of Electrochemistry, 54, 860–866.

Shi Y., Wang J., Li S., Yan B., Xu H., Zhang K., Du Y., 2017, The Enhanced Photo-Electrochemical Detection of Uric Acid on Au Nanoparticles Modified Glassy Carbon Electrode, Nanoscale Research Letters 12, 455.

Struck W.A., Elving P.J., 1965, Electrolytic Oxidation of Uric Acid: Products and Mechanism, Biochemistry, 4, 1343–1353.

Temmer R., Maziz A., Plesse C., Aabloo A., Vidal F., Tamm T., 2013, In search of better electroactive polymer actuator materials: PPy versus PEDOT versus PEDOT–PPy composites, Smart Materials and Structures, 22, 104006.

Tukimin N., Abdullah J., Sulaiman Y., 2017, Development of a PrGO-Modified Electrode for Uric Acid Determination in the Presence of Ascorbic Acid by an Electrochemical Technique, Sensors, 17, 1539.

Wu Y., Deng P., Tian Y., Feng J., Xiao J., Li J., Liu J., Li G., He Q., 2020, Simultaneous and sensitive determination of ascorbic acid, dopamine and uric acid via an electrochemical sensor based on PVP-graphene composite, Journal of Nanobiotechnology, 18, 112.

Xia Y., Xiang Q., Gu Y., Jia S., Zhang Q., Liu L., Meng G., Wu H., Bao X., Yu B., Sun S., Wang X., Zhou M., Jia Q., Wu Y., Song K., Niu K., 2018, A dietary pattern rich in animal organ, seafood and processed meat products is associated with newly diagnosed hyperuricaemia in Chinese adults: a propensity score-matched case–control study, British Journal of Nutrition, 119, 1177–1184.

Xue Y., Zhao H., Wu Z., Li X., He Y., Yuan Z., 2011, The comparison of different gold nanoparticles/graphene nanosheets hybrid nanocomposites in electrochemical performance and the construction of a sensitive uric acid electrochemical sensor with novel hybrid nanocomposites, Biosensors and Bioelectronics, 29, 102–108.

Yazdani M., Yazdani A., Noori-Mahdavi K., Kabiri M., Baradaran S., Nasri H., 2015, Serum and 24-Hour Urinary Uric Acid Levels in Patients with Urolithiasis, Shiraz E-Medical Journal 16.